

## Influence of Impurities on the Solubility, Nucleation, Crystallization and Compressibility of Paracetamol

Leila Keshavarz, René R. E. Steendam, Melian A.R. Blijlevens, Mahboubeh Pishnamazi, and Patrick J. Frawley

*Cryst. Growth Des.*, **Just Accepted Manuscript** • Publication Date (Web): 22 May 2019

Downloaded from <http://pubs.acs.org> on May 30, 2019

### Just Accepted

“Just Accepted” manuscripts have been peer-reviewed and accepted for publication. They are posted online prior to technical editing, formatting for publication and author proofing. The American Chemical Society provides “Just Accepted” as a service to the research community to expedite the dissemination of scientific material as soon as possible after acceptance. “Just Accepted” manuscripts appear in full in PDF format accompanied by an HTML abstract. “Just Accepted” manuscripts have been fully peer reviewed, but should not be considered the official version of record. They are citable by the Digital Object Identifier (DOI®). “Just Accepted” is an optional service offered to authors. Therefore, the “Just Accepted” Web site may not include all articles that will be published in the journal. After a manuscript is technically edited and formatted, it will be removed from the “Just Accepted” Web site and published as an ASAP article. Note that technical editing may introduce minor changes to the manuscript text and/or graphics which could affect content, and all legal disclaimers and ethical guidelines that apply to the journal pertain. ACS cannot be held responsible for errors or consequences arising from the use of information contained in these “Just Accepted” manuscripts.

1  
2  
3 **Influence of Impurities on the Solubility, Nucleation, Crystallization and Compressibility of**  
4  
5 **Paracetamol**  
6  
7  
8

9 **Leila Keshavarz<sup>1†\*</sup>, René R. E. Steendam<sup>1†</sup>, Melian A. R. Blijlevens<sup>1</sup>, Mahboubeh Pishnamazi<sup>2</sup>**  
10 **and Patrick J. Frawley<sup>1</sup>**  
11  
12  
13  
14  
15  
16  
17

18 <sup>1</sup> Department of Mechanical & Aeronautical Engineering, Bernal Institute, Synthesis and Solid State  
19 Pharmaceutical Centre (SSPC), University of Limerick, Limerick, Ireland  
20  
21

22 <sup>2</sup> Department of Chemical Sciences, Bernal Institute, Synthesis and Solid State Pharmaceutical Centre  
23 (SSPC), University of Limerick, Limerick, Ireland  
24  
25  
26  
27

28 † Equal contribution  
29

30 \* Corresponding author  
31  
32  
33  
34

35 **ABSTRACT**

36 The striking ability of impurities to significantly influence crystallization processes is a topic of  
37 paramount interest in the pharmaceutical industry. Despite being present in small quantities,  
38 impurities tend to considerably change a crystallization process as well as the final crystalline product.  
39 In the present work, the effect of two markedly different impurities 4-nitrophenol and 4'-  
40 chloroacetanilide on the solubility, nucleation and crystallization of paracetamol are described. In the  
41 first part of this work, the fundamentals are outlined and show that although each impurity led to a  
42 small increase in solubility of paracetamol, their effect as a nucleation inhibitor was much more  
43 pronounced. Induction time experiments were used in conjunction with the classical nucleation theory  
44 to show that the impurities did not affect the solid-liquid interfacial energy but instead significantly  
45 reduced the kinetic factor, overall resulting in reduced nucleation rates. Intriguingly, both impurities  
46 influenced the solubility and nucleation of paracetamol in a similar fashion despite their significant  
47 differences in terms of molecular structure, solubility and ability to incorporate into the crystal  
48  
49  
50  
51  
52  
53  
54  
55  
56  
57  
58  
59  
60

1  
2  
3 structure of paracetamol. In the second part of this work, the incorporation of 4'-chloroacetanilide into  
4 the solid phase of paracetamol was investigated. The presence of 4'-chloroacetanilide in the solid  
5 phase of paracetamol significantly increased the compressibility of paracetamol, resulting in improved  
6 processability properties of paracetamol. The compressibility efficiency of paracetamol could be  
7 controlled using the amount of incorporated 4'-chloroacetanilide. Therefore, an experimental design  
8 space was developed and utilized to select the most important process parameters for impurity  
9 incorporation. Intriguingly, the number of carbon atoms in the aliphatic chain of the alcohol solvent  
10 strongly correlated to the impurity incorporation efficiency. As a result, it was feasible to accurately  
11 control the compressibility and the amount of 4'-chloroacetanilide in the solid phase of paracetamol  
12 by simply choosing the required alcohol as the solvent for crystallization. Thus, the present work  
13 comprehensively shows how different impurities impact the key crystallization mechanisms and  
14 properties of a pharmaceutical product. Rational process control over the incorporation of impurities  
15 and additives allows for advanced manufacturing of products with tailored specifications.

## 31 1. INTRODUCTION

32  
33  
34 Solution crystallization processes are widely treated as binary systems consisting of a solute  
35 and a solvent. For real systems, additional components such as additives and impurities are typically  
36 present in minute amounts. Such additional components may significantly impact crystallization  
37 processes even when present in very small amounts.<sup>1, 2</sup> An understanding of the mechanistic role of  
38 additives and impurities is therefore essential to design and control crystallization processes. Impurity  
39 control is particularly important in pharmaceutical manufacturing, as such compounds can be toxic or  
40 may unfavourably affect the crystallization of the desired product.<sup>3, 4</sup>

41  
42  
43 Impurities influence crystallization processes in several ways.<sup>5, 6</sup> For instance, the solubility of  
44 the product can change as a result of a change in the solute-solvent interfacial energy due to the  
45 presence of additional components. Consequently, the solubility of the product may decrease due to  
46 the presence of common ions or increase as a result of complex formation or the presence of foreign  
47 ions.<sup>1</sup> Impurities furthermore may influence the nucleation process by changing the solid-liquid  
48 interfacial energy<sup>7</sup> and/or the kinetic factor or they may act as heterogeneous surfaces.<sup>1, 8</sup> For instance,  
49  
50  
51  
52  
53  
54  
55  
56  
57  
58  
59  
60

1  
2  
3 amphiphilic, polymeric and surfactant additives were found to promote nucleation.<sup>9-11</sup> In other studies  
4 it was found that additives and impurities did not significantly influence the interfacial energy but  
5 instead led to a reduction in the kinetics.<sup>12, 13</sup> These findings were explained using the additional  
6 energy that is required to remove the impurity from the clustering process. Finally, additives can be  
7 used to influence the processability of pharmaceutical compounds by changing the intrinsic physical  
8 properties. For example, additives were found to increase the compressibility of paracetamol which  
9 enabled enhanced direct compression resulting in stronger tablets.<sup>14, 15</sup>

10  
11  
12 Paracetamol (PA, Figure 1) is widely used as an over-the-counter analgesic and antipyretic  
13 painkiller. Three polymorphic forms of PA have been reported, of which Form I is the most stable  
14 form at room temperature.<sup>16-18</sup> To date, the effect of a range of structurally-related compounds have  
15 been studied as additives on the crystallization of PA.<sup>19-22</sup> However, it remains unclear how the main  
16 impurities 4-nitrophenol (NP) and 4'-chloroacetanilide (CA) affect the solubility, nucleation and  
17 crystallization of PA (Figure 1). The synthesis of paracetamol typically involves the reduction of NP  
18 into 4-aminophenol which in turn is used as the final precursor to paracetamol. NP can be obtained  
19 through the *p*-nitrochlorobenzene route, in which unreacted *p*-nitrochlorobenzene forms impurity CA  
20 parallel to the desired synthesis route.<sup>24</sup> CA is not a hazardous substance and as such may be used as  
21 an additive.<sup>25</sup> Understanding the mechanisms by which additional compounds influence  
22 crystallization is of great interest to the scientific community and would allow for more controlled and  
23 robust crystallization processes.<sup>3</sup>

24  
25  
26 Herein, the influence of impurities NP and CA on the crystallization of PA are reported. In  
27 the first part of this work, the effect of NP and CA on the solubility and crystal nucleation of PA is  
28 described. Equilibrium solubility experiments in combination with high pressure liquid  
29 chromatography (HPLC) analysis was used to determine the solubility increase of PA as a result of  
30 impurity NP and CA. The crystal nucleation mechanisms were elucidated by combining the data of  
31 more than 1000 isothermal induction time experiments with the classical nucleation theory (CNT). In  
32 the second part of this work, the ability of impurity CA to incorporate into the solid phase of PA was  
33 studied. Compressibility studies were performed for pure PA crystals as well as PA crystals doped  
34 with CA. The compressibility of PA significantly depended on the amount of CA in the crystal

1  
2  
3 structure. Therefore, a statistical fractional factorial design approach was utilized to determine which  
4 factors most significantly controlled the impurity incorporation process.<sup>26</sup> The type of solvent was one  
5 of the most important factors that affected the impurity incorporation and as such was investigated in  
6 more detail by testing alcohols with varying carbon chain lengths as solvents for crystallization.  
7  
8  
9

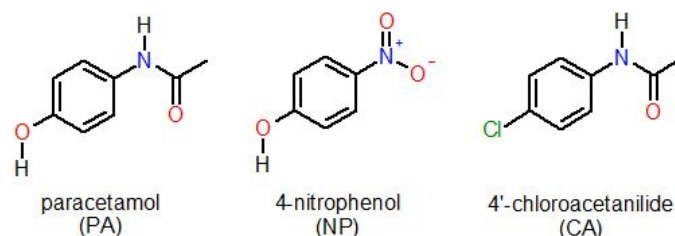


**Figure 1.** The molecular structures of paracetamol (PA) and impurities 4-nitrophenol (NP) and 4'-chloroacetanilide (CA).

## 2. EXPERIMENTAL

### 2.1. Materials

PA (98.0-102.0%) was purchased from Sigma-Aldrich whereas NP (99%) and CA (98+%) were obtained from Alfa Aesar. The solvents methanol, ethanol, 1-propanol, 2-propanol, 1-butanol, 1-pentanol, 1-hexanol and 1-octanol were obtained from Sigma-Aldrich. HPLC-grade water was obtained using a PURELAB flex 3 purification instrument. All chemicals and solvents were used as received. Seed crystals of PA were acquired through recrystallization of PA from methanol at a slow cooling rate of 0.1 °C/min at a stirring rate of 300 rpm in a Mettler Toledo Easymax 402 setup. The seed crystals were sieved and a size range of 180-250 μm was used in the experiments.

The solids obtained at the end of the experiments were analyzed using X-Ray Powder Diffraction (XRPD) to ensure that no polymorphic transformations occurred. A PANalytical EMPYREAN diffractometer with Bragg–Brentano geometry and an incident beam of Cu K-Alpha radiation ( $\lambda = 1.5406 \text{ \AA}$ ) was used for the XRPD measurements. A spinning silicon sample holder was used and the analysis was performed at room temperature with a step size of  $0.013^\circ 2\theta$  and a step time of 68 s.

### 2.2. Solubility Determination

1  
2  
3 The solubility of PA in the presence of impurities was determined through a previously  
4 reported gravimetric method in combination with HPLC analysis.<sup>27</sup> For these experiments, 2-propanol  
5 was used as a representative solvent because of its low cost in combination with favourable  
6 environmental, health and safety properties.<sup>28</sup> A solid mixture consisting of 2.0 g of PA and 5 mol%  
7 of either NP or CA was added to 2-propanol. The resulting suspension was heated until the solids  
8 were completely dissolved after which the solution was brought down to the solubility temperature for  
9 solubility determination. The suspension was stirred for a minimum of 24 h after which three samples  
10 from the filtered solid-free supernatant were removed, weighted and dried. The resulting solids were  
11 analysed using HPLC to determine the ratio of PA to NP or CA.  
12  
13  
14  
15  
16  
17  
18  
19  
20  
21  
22

### 23 **2.3. Induction Time Measurements**

24  
25 A solution of PA in 2-propanol was prepared with supersaturation ratios  $S=1.4, 1.6, 1.8$  and  
26 2.0. In order to minimize variations between the eight vials, a stock solution was prepared in 100 mL  
27 2-propanol. 1 mol% of either CA or NP was added to the stock solution. The supersaturation ratios  $S$   
28 were calculated with solubility data reported in literature.<sup>29</sup> Crystallization was carried out at a  
29 temperature  $T$  of 5 °C. For supersaturation ratios  $S=1.4, 1.6, 1.8$  and 2.0 the stock solutions were  
30 heated for half an hour at 30 °C, 40 °C, 50 °C and 50 °C, respectively. The stock solution was filtered  
31 using Whatman filter paper (25 µm pore size) to remove particulates larger than 25 µm. 10 mL was  
32 taken from the stock solution and transferred using a 5 mL micropipette into 20 mL vials. The vials  
33 were heated for another half hour at their respective temperatures and were subsequently placed in a  
34 thermostated waterbath (Grant GR150; 38L; stability  $\pm 0.005$  K; uniformity  $\pm 0.02$  K) which was set at  
35 a temperature of 5 °C. The time required to reach the set temperature was recorded and used as the  
36 start time of the experiment. Each vial contained a 10 mL solution and a cross-shaped stirrer bar  
37 ( $\phi=18$  mm) and the vials were closed with a screw cap. The vials were placed on a submersible stirrer  
38 plate (2mag MIXdrive 1) and the stirrer speed was kept constant at 350 rpm. The experiments were  
39 recorded with a Logitech Quickcam USB camera. Stirring continued until the clear solution turned  
40 opaque, which indicated the onset of crystallization. The time difference between the onset of  
41 crystallization and the solution reaching the set temperature was taken as the crystallization time.  
42  
43  
44  
45  
46  
47  
48  
49  
50  
51  
52  
53  
54  
55  
56  
57  
58  
59  
60

## 2.4. Crystallization Experiments

The cooling crystallization experiments for the fractional factorial design were carried out in a Mettler Toledo Easymax 402 setup. Mixing was performed using an overhead stirrer with a downward pitched-blade stirrer ( $\phi = 25$  mm). The stirring rate was set at either 300 rpm or 400 rpm. PA (62.8 g) and CA (1.4 g, 2 mol%) were mixed with 2-propanol (235.8 g) and heated to 70 °C for an hour to ensure complete dissolution of the solids. Once dissolved, the temperature  $T$  of the solution was decreased to 15 °C during a cooling time of either 550 min or 61 min to reach a supersaturation ratio  $S=2.82$ . For the experiments in ethanol, PA (98.9 g) and CA (2.3 g, 2 mol%<sup>30</sup>) were mixed with ethanol (235.8 g). The same process parameters used in the 2-propanol experiments were applied in the ethanol experiments. For the experiments in ethanol the supersaturation ratio was  $S=2.5$ .

The cooling method was programmed to proceed either linearly or through temperature cycles (Figure 2). Both cooling methods were tested as a linear cooling approach is perhaps more commonly applied in industry whereas temperature cycles lead to changes in product properties and possibly higher product purities.<sup>31</sup> Seed crystals (2 wt%) were added at a temperature of  $T=50$  °C in the seeded experiments. After the cooling programme was finished, the suspension was mixed at a temperature  $T=15$  °C for a minimum of 48h to ensure complete desupersaturation. The suspension was subsequently filtered and the solids were dried in an oven set at a temperature  $T=50$  °C. A sample of the resulting dried solids was analyzed using HPLC to determine the ratio of PA to CA.

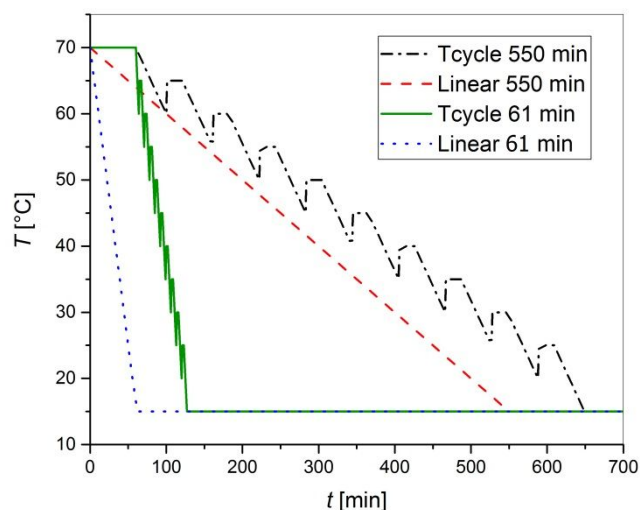


**Figure 2.** Cooling profiles used for the cooling crystallization experiments.

Experiments to study the effect of different alcohols were performed in 20 mL vials equipped with cross-shaped stirrer bars ( $\phi=18$  mm). The vials were closed with a screw cap and placed on a submersible stirrer plate (2mag MIXdrive 1) inside of a thermostated waterbath (Grant GR150; 38L; stability  $\pm 0.005$  K; uniformity  $\pm 0.02$  K). The applied stirring rate was 500 rpm. PA and CA (2 mol%) were combined with each alcohol and the suspensions were mixed at 10 °C above their saturation temperatures at 40 °C for 1 h to ensure complete dissolution of the solids. The temperature of the resulting clear solutions was reduced during a cooling time of 550 min to a crystallization temperature that would induce supersaturation ratio  $S=1.7$  for all experiments.

Crystals for the compressibility studies were obtained from cooling crystallization in a Mettler Toledo Easymax 402 setup. PA (62.8 g) was combined with either 1 mol% or 2 mol% of CA in 2-propanol (235.8 g). A clear solution was obtained by stirring the suspension at 400 rpm at a temperature  $T=70$  °C for 1 h. Once dissolved, the temperature of the solution was linearly reduced to 15 °C during a cooling time of 61 min. Stirring continued at a temperature  $T=15$  °C for a minimum of 48 h to ensure complete desupersaturation after which the solids were isolated through filtration, dried at temperature  $T=50$  °C and used for the compressibility study. A small sample was taken from the solids and subjected to HPLC analysis.

## 2.5. HPLC Analysis

The ratio of PA to either NP or CA was determined using a High Pressure Liquid Chromatography (HPLC) methodology based on previous studies.<sup>32, 33</sup> An Agilent 1260 Infinity Quaternary LC instrument was used that was equipped with a ZORBAX eclipse XDB-C18 column (4.6x150 mm, 3.5 $\mu$ ). The mobile phase consisted of a 0.01 M sodium phosphate buffer (pH=3) and methanol in a ratio of 0.8/0.2 (v/v) or 1/1 (v/v), for PA/CA or PA/NP, respectively. For the 0.8/0.2 (v/v) mobile phase, the retention times for PA and CA were 1.48 min and 2.10 min, respectively. Using the 1/1 (v/v) mobile phase, the retention times of 1.72 min and 4.58 min were assigned to PA



1  
2  
3 and NP, respectively. The applied flowrate was 1 mL/min, the column temperature was set to 20 °C  
4  
5 and the injection volume was 5 µL. PA and CA were measured at a wavelength of 254 nm whereas  
6  
7 NP was measured at a wavelength of 310 nm. The solid phase samples were dissolved in methanol  
8  
9 and added to 2 mL amber borosilicate glass vials. Calibrations lines of at least 10 concentration points  
10  
11 were measured for PA, CA and NP and each concentration was measured in triplicate. The resulting  
12  
13 low standard deviation of <1% for each sample reflects the accuracy of the analytical procedure.  
14  
15 Using the linear calibration lines, which are reported in literature<sup>33</sup>, it was feasibly to determine the  
16  
17 ratio of PA to either NP or CA of unknown samples.  
18  
19  
20  
21

## 22 **2.6. Compressibility Studies**

23  
24 The compaction behaviour of the materials was studied using a powder flow rheometer  
25  
26 (Freeman Technologies FT4) which was used to measure the compressibility.<sup>34</sup> A vented piston was  
27  
28 used as a standard measurement method in order to compact powder by applying a normal stress.  
29  
30 During the test, the range of normal stress was varied between 1-2-4-6-8-10-12-15 kPa.  
31  
32  
33  
34

## 35 **3. RESULTS AND DISCUSSION**

36  
37 The first part of the results describes the fundamentals as to how impurities CA and NP  
38  
39 influence the solubility and crystal nucleation of PA. In these experiments, 2-propanol was used as the  
40  
41 solvent. Impurity CA incorporates into the solid phase of PA whereas NP remained in solution and  
42  
43 did not affect the solid phase of PA.<sup>32, 35</sup> In the second part of the results, the ability of CA to  
44  
45 incorporate into the solid phase of PA was used to tailor the solid phase of PA and to improve its  
46  
47 product properties. A statistical design approach was utilized to learn which process factors control  
48  
49 the incorporation of impurity CA and with that the compressibility of PA.  
50  
51  
52  
53

### 54 **3.1. Fundamentals**

#### 55 **3.1.1. Solubility**

56  
57  
58  
59  
60

Both PA and NP may form different polymorphs whereas only one form of CA has been reported to date. In a previous study it was established that Form I of PA and the  $\alpha$ -form of NP were used and both forms remained stable across a temperature range of 5-55 °C in various alcohols.<sup>33</sup> The same conditions were used in the present study and XRPD analyses showed that the initial polymorphic form of the compounds were retained throughout the experiments. The solubility of CA was previously found to be slightly lower than the solubility of PA whereas NP has an approximate 10-fold higher solubility than PA.<sup>33</sup>

In the current work, the solubility  $C^*$  of PA in the presence of either 5 mol% of NP or 5 mol% of CA was determined across a temperature range of 5-55 °C. Figure 3 shows that the solubility of PA slightly increased due to the presence of CA or NP across the tested temperature range. Despite the significant differences between NP and CA in terms of solubility and molecular structure, each compound increased the solubility of PA in a similar way. A similar small solubility increase of PA was observed for additives metacetamol and acetanilide.<sup>22</sup> Overall, the presence of either NP or CA did not significantly affect the solubility of PA.

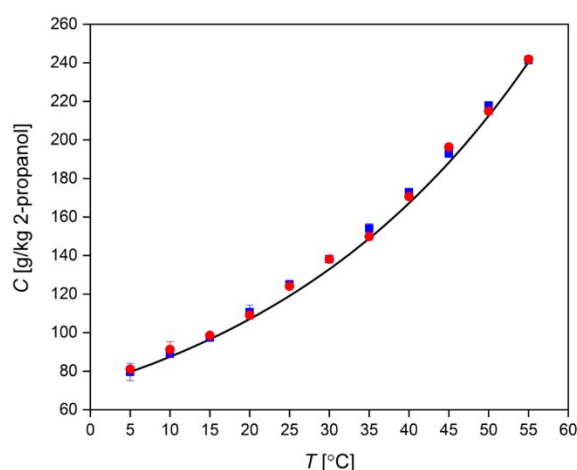


**Figure 3.** Solubility  $C^*$  of PA in the presence of 5 mol% NP (●) and 5 mol% CA (■) in 2-propanol as a function of temperature  $T$ . The line represents the solubility of pure PA in 2-propanol calculated using the Apelblat parameters reported in literature.<sup>36</sup>

### 3.1.2. Crystal Nucleation

1  
2  
3 The influence of impurities NP and CA on the crystal nucleation of PA in 2-propanol was  
4 investigated using induction time measurements in combination with the classical nucleation theory  
5 (CNT).<sup>37-39</sup> Figure 4a-c shows probability distributions of induction times  $t_i$  for pure PA and PA in the  
6 presence of either 1 mol% of NP or 1 mol% of CA for different supersaturation ratios  $S$ . The  
7 supersaturation ratio  $S$  is defined as  
8  
9  
10  
11  
12

$$13 S = \frac{C}{C^*} \quad (1)$$

14  
15  
16  
17  
18  
19  
20 where  $C$  is the total concentration and  $C^*$  is the equilibrium solution concentration at the set  
21 temperature, both expressed in g per kg solvent. For each supersaturation ratio  $S$ , the dataset was fitted  
22 to the following equation  
23  
24  
25

$$26 P(t_i) = 1 - \exp(-JVt_i) \quad (2)$$

27  
28  
29  
30  
31  
32  
33 where  $P$  represents the probability that at least one nucleus has formed in volume  $V$  and  
34 where  $J$  represents the nucleation rate in  $\text{m}^{-3} \cdot \text{s}^{-1}$ . On average, the quality of fit of eq. 2 to the data was  
35 sufficiently high ( $R^2 = 0.96$ ). The induction time  $t_i$  of a nucleus could not be measured directly but  
36 could be estimated as follows  
37  
38  
39  
40  
41

$$42 t_i = t_c - t_g \quad (3)$$

43  
44  
45  
46  
47  
48  
49 where  $t_c$  is the time of crystallization and  $t_g$  the growth time of a nucleus. The growth time  $t_g$   
50 of a nucleus was taken as a parameter from fitting eq. 1 to the experimental data. The time required to  
51 reach the set temperature of 5 °C after placing the vials in the waterbath starting from a temperature  
52 30 °C, 40 °C and 50 °C was 211 s, 230 s and 243 s, respectively. These cooling times were subtracted  
53  
54  
55  
56  
57  
58  
59  
60 from the detection time to obtain the time of crystallization  $t_c$ .

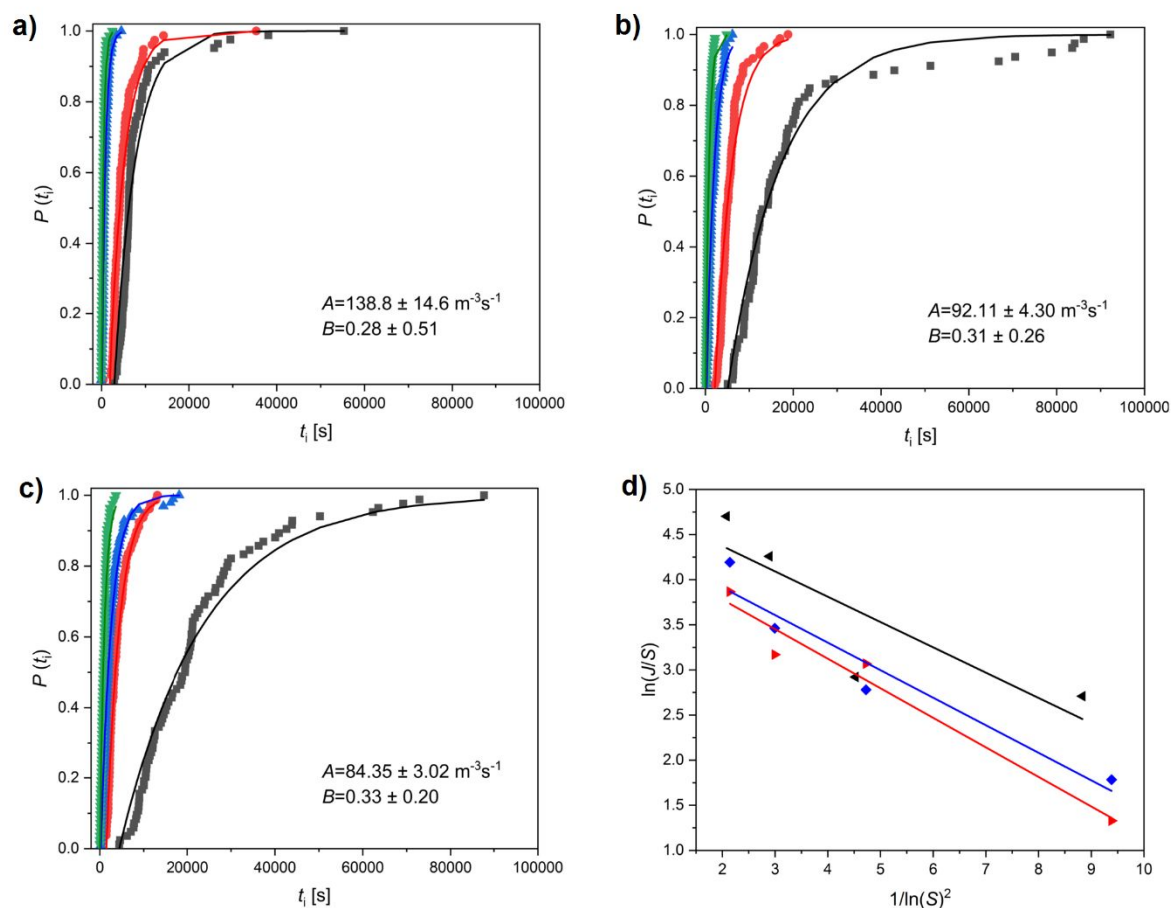


**Figure 4.** Probability distributions  $P(t)$  of induction times  $t_i$  measured at supersaturation ratios  $S = 1.4$  (■), 1.6 (●), 1.8 (▲) and 2.0 (▼) in 2-propanol for pure PA (a) and PA in the presence of 1 mol% CA (b) and 1 mol% NP (c). A plot of  $\ln(J/S)$  versus  $1/\ln(S)^2$  is depicted in (d) for the pure PA experiments (◄) as well as the experiments involving impurities CA (◆) and NP (►). From the linear fits, parameters  $A$  and  $B$  from eq. 4 were estimated and are shown in Figures a-c with 95% confidence limits.

The nucleation rate  $J$  is plotted in Figure 5a as a function of supersaturation ratio  $S$  for the pure and impure systems. Except for supersaturation ratio  $S=1.6$ , the nucleation rate  $J$  of PA is significantly inhibited by both impurities CA and NP. Previous studies showed that the structurally-related impurities metacetamol and *p*-acetoxyacetanilide also inhibit the nucleation rate of PA.<sup>20, 21</sup> On average and across the tested supersaturation ratio  $S$  range, the nucleation rate  $J$  of PA was reduced by a factor of 1.9 or 2.6 due to the presence of 1 mol% impurity CA or NP, respectively. Therefore, NP

inhibits the nucleation rate  $J$  of PA more efficiently than CA. Both impurities inhibit the development of the PA clusters, which is reflected by the longer growth times  $t_g$  of the impure nuclei with respect to pure PA (Figure 5b). With increasing supersaturation ratios  $S$ , the factor between the nucleation rate  $J$  and growth time  $t_g$  of the pure and impure systems increases.

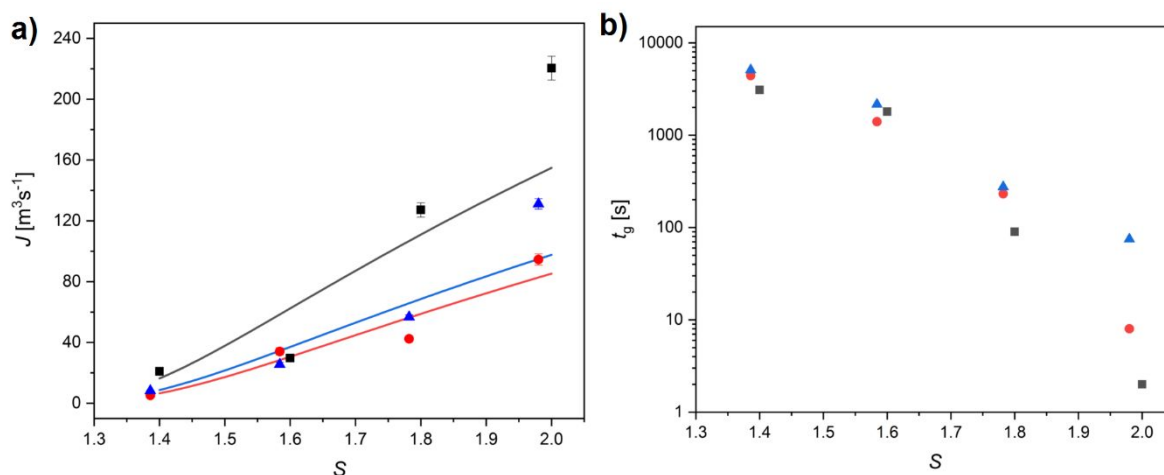


**Figure 5.** Nucleation rate  $J$  (a) and the growth time  $t_g$  of a nucleus (b) as a function of supersaturation ratio  $S$  for pure PA (■) and PA in the presence of 1 mol% CA (▲) and 1 mol% NP (●) in 2-propanol. The nucleation rate  $J$  data points contain 95% confidence limits and the lines are plots of eq. 4.

The nucleation rate expression was inspected in more detail to understand the mechanism by which the impurities inhibit the development of the nuclei. According to the CNT, the nucleation rate  $J$  depends on the supersaturation ratio  $S$ , kinetic parameter  $A$  and thermodynamic parameter  $B$ , as shown in eq. 4

$$J = AS \exp\left(-\frac{B}{\ln^2 S}\right) \quad (4)$$

A fit of the linearized form of eq. 4 through a least-squares approach yield parameter  $\ln(A)$  from the intercept and parameter  $B$  from the slope (Figure 4d). The linear fits to the impure systems ( $R^2=0.93$  for CA and 0.96 for NP) were better than the linear fit to the pure system ( $R^2=0.74$ ).

1  
2  
3 The values for parameters  $A$  and  $B$  of each system are shown in the corresponding plots in  
4 Figure 4. The differences between the values of thermodynamic parameter  $B$  of each system are  
5 virtually the same, showing that the presence of either CA or NP does not significantly change the  
6 interfacial energy of the crystal/solution interface of the system. In contrast, the presence of either CA  
7 or NP significantly lowered the kinetic parameter  $A$  by a factor of 1.5 or 1.6, respectively. Kinetic  
8 parameter  $A$  can be described through the CNT as  
9  
10  
11  
12  
13  
14

$$15 A = zf^* C_0 \quad (5)$$

16  
17  
18 with  $z$  representing the Zeldovich factor which accounts for clusters that decay rather than grow into  
19 stable crystals,  $f^*$  accounting for the attachment frequency of monomers to the nucleus and  $C_0$   
20 accounting for the concentration of nucleation sites.<sup>40</sup> Nucleation sites are typically considered as  
21 heterogeneous surfaces that promote heterogeneous nucleation.  
22  
23  
24  
25  
26  
27  
28  
29

30 As discussed in a previous study, the Zeldovich factor  $z$  depends on the supersaturation ratio,  
31 Boltzmann constant, temperature, molecular volume in the crystal and the interfacial energy and these  
32 values are unlikely to change due to the presence of impurities.<sup>10</sup> Instead, impurities may interact with  
33 nucleation interfaces, effectively lowering the concentration of nucleation sites  $C_0$  for PA. The nature  
34 of the nucleation sites is unknown and therefore the exact mechanism by which heterogeneous  
35 nucleation occurs remains elusive. One way of obtaining more insight into the mechanism by which  
36 nucleation sites induce nucleation is by controlling the nucleation sites using well-defined templates.<sup>41</sup>  
37  
38  
39  
40  
41  
42  
43  
44

45 The second parameter in eq. 5 that may be influenced by the presence of impurities is the  
46 attachment frequency of building units to the nucleus  $f^*$ , which can be expressed through  
47  
48  
49  
50

$$51 f^* = \lambda A^* D \frac{X_1}{d} \quad (6)$$

52  
53  
54  
55  
56 where  $\lambda$  is the sticking coefficient that accounts for building units near the cluster which are not  
57 incorporated into the nucleus,  $A^*$  is the nucleus surface area,  $D$  is the diffusion coefficient,  $X_1$  is the  
58  
59  
60

1  
2  
3 concentration of building units and  $d$  is the diameter of the nucleus. The diffusion coefficient  $D$  is  
4 perhaps the most important parameter to be affected by impurities as it depends on the activation  
5 energy  $E$  through  
6  
7  
8  
9

$$10 \quad D = D_0 e^{-E/RT} \quad (7)$$

11  
12  
13  
14  
15 in which  $R$  is the gas constant,  $D_0$  the diffusion constant and  $T$  the absolute temperature.<sup>40</sup> The  
16 activation energy  $E$  accounts for the energy barrier required for a molecule to undergo desolvation  
17 and/or to undergo a conformational change during incorporation of a growing nucleus.  
18  
19  
20  
21

22 It was previously found using HPLC that impurity NP does not incorporate into the crystal  
23 structure of PA.<sup>32,33</sup> The inability of NP to incorporate into the crystal structure of PA may be due to  
24 its strong hydrogen bond forming capability which would lead to strong hydrogen bonds with solvent  
25 2-propanol, as evidenced by the high solubility of NP in alcohols. Therefore, impurity NP may affect  
26 the conformational change of PA molecules into the growing nucleus and/or influence the desolvation  
27 process of PA. A previous report explained the inhibiting effect of impurities on kinetic parameter  $A$   
28 to a higher energy barrier that needed to be passed in order to remove the impurities from a growing  
29 nucleus.<sup>12</sup> This extra energy requirement may be considered as the activation energy  $E$  in eq. 7 and  
30 may explain the inhibiting effect of NP on PA as well. Furthermore in related work, the inhibiting  
31 effect of a dilute hydrogen-bonding additive on the nucleation of a small molecule was explained  
32 using the two-step nucleation theory, in which the impurity inhibits the kinetic ordering of the  
33 transition of a high-density cluster into an ordered crystal structure.<sup>13</sup> The same principles may apply  
34 to the inhibiting effects of NP on PA as a decrease in kinetic parameter  $A$  was observed in the present  
35 work as well. Both the diffusion coefficient  $D$  in the CNT as well as the kinetic ordering parameter in  
36 the two-step nucleation theory may be influenced by impurities and therefore it remains unclear  
37 through which mechanism nucleation proceeds in the present work.  
38  
39  
40  
41  
42  
43  
44  
45  
46  
47  
48  
49  
50  
51  
52  
53  
54

55 In the case of impurity CA, the mechanism by which the impurity inhibits nucleation of PA is  
56 strikingly different to NP and previous findings. This is because impurity CA incorporates and  
57 remains in the crystal structure of PA. The OH-group in PA is a key functional group in PA Form I as  
58  
59  
60

1  
2  
3 it acts as a hydrogen bond donor and acceptor, leading to hydrogen bonds with two different  
4 neighbouring molecules.<sup>42</sup> However, impurity CA lacks an OH-group and therefore restricts the  
5 possibilities of new PA building units to incorporate into the growing nucleus. Therefore, more time is  
6 needed for PA building units to adopt the required limited configuration possibilities to incorporate  
7 into the nucleus, leading to a higher activation energy  $E$  as a result of CA. On the other hand, the  
8 inhibiting effect may also be explained using the two-step nucleation theory as CA may affect the  
9 kinetic ordering of a high-density cluster into an ordered crystal structure, thereby lowering kinetic  
10 parameter  $A$ . As with impurity NP it remains elusive whether nucleation in the present work proceeds  
11 through the CNT or through a liquid-like intermediate in the two-step nucleation theory.  
12  
13  
14  
15  
16  
17  
18  
19  
20  
21  
22  
23

## 24 **3.2. Tailoring Product Properties**

### 25 **3.2.1. Compressibility**

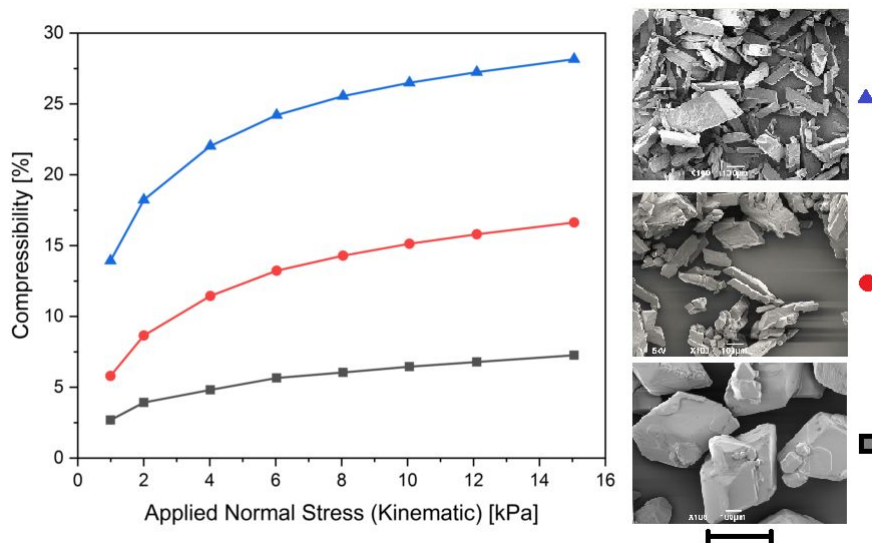
26  
27  
28  
29  
30  
31 Compressibility is an important parameter for pharmaceutical formulations that can influence  
32 tableability of powders and the properties of prepared tablets such as hardness and disintegration  
33 time.<sup>34</sup> The density of powder is considered as a function of applied normal stress and compressibility  
34 is typically described as a function of density variability. Therefore, compressibility is the volume  
35 reduction of powders as a result of the applied normal stress.  
36  
37  
38  
39  
40

41  
42  
43  
44  
45  
46  
47  
48  
49  
50  
51  
52  
53  
54  
55  
56  
57  
58  
59  
60  
PA Form I, which has been used throughout this study, is known for its poor flowability and  
capping tendency upon compression. One approach to increase the compressibility of pharmaceuticals  
is through the use of additives, as the presence of additives typically leads to less efficient crystal  
packing and more open crystal structures. Such an open structure would favour direct compression,  
resulting in stronger tablets. Polymer additives have been used in previous studies to enhance the  
compressibility of PA.<sup>14, 15</sup>

In the present work, the small molecule CA was used to increase the compressibility of PA.  
Figure 6 shows the compressibility as a function of normal stress for pure PA crystals as well as PA  
crystals doped with either 0.47 mol% or 0.73 mol% CA. Interestingly, the presence of only a minute  
amount of CA induced a striking increase in compressibility with respect to pure PA. At an applied



1  
2  
3 stress of 15 kPa, the compressibility of pure PA was only 7.26% whereas it significantly increased to  
4 16.63% and 28.16% due to the presence of 0.47 mol% and 0.73 mol% CA, respectively. The  
5 incorporation of CA into the solid phase of PA also led to a significant change in crystal habit (Figure  
6 6). Instead of tabular crystals, impurity CA induced the formation of needle-shaped crystals of PA.  
7  
8  
9  
10  
11 Thus, impurity CA can be used to significantly favour the compressibility of PA, even when present  
12  
13  
14 in a very small amount.



37  
38 **Figure 6.** a) Compressibility as a function of normal stress and SEM images of the starting materials  
39 of pure PA crystals (■) and PA crystals containing 0.47 mol% CA (●) and 0.73 mol% CA (▲) which  
40 were used for the compressibility study. The size bar represents 300 μm.  
41  
42  
43  
44  
45  
46  
47

### 48 3.3.1. Parameter Screening

49  
50 As illustrated in the previous paragraph, the compressibility of PA significantly depends on  
51 the amount of CA that is present in the solid phase of PA. Accurately controlling the amount of CA  
52 that becomes incorporated into the solid phase of PA is therefore essential to tailor the desired product  
53 specifications of PA. The applied experimental conditions typically control the incorporation of  
54 impurities into the solid phase of a product.<sup>43</sup> However, it is unclear how the wide variety of  
55  
56  
57  
58  
59  
60

experimental factors influence the incorporation of CA into the solid phase of PA. Therefore, a series of cooling crystallization experiments were performed to determine which factors most significantly control the impurity incorporation of CA into PA. The five factors that were investigated were the type of cooling method (linear or temperature cycles, Figure 2), cooling time (61 min or 550 min), stirring rate (300 rpm or 400 rpm), seeding (yes or no) and solvent type (2-propanol or ethanol). Instead of testing all the possible combinations of these factors, a fractional factorial approach in Minitab software was utilized to design a  $2^{5-1}$  work space involving 16 experiments with resolution V.

**Table 1.** Overview of the Experiments Designed Using a Fractional Factorial Approach.<sup>a</sup>

entry	cooling method	cooling time [min]	stirring rate [rpm]	seeding	solvent	PA [%] <sup>b</sup>
1	linear	61	300	no	ethanol	99.10
2	cycles	61	300	no	2-propanol	99.22
3	linear	550	300	no	2-propanol	99.43
4	cycles	550	300	no	ethanol	99.08
5	linear	61	400	no	2-propanol	99.27
6	cycles	61	400	no	ethanol	99.37
7	linear	550	400	no	ethanol	99.37
8	cycles	550	400	no	2-propanol	99.37
9	linear	61	300	yes	2-propanol	99.31
10	cycles	61	300	yes	ethanol	96.45
11	linear	550	300	yes	ethanol	99.20
12	cycles	550	300	yes	2-propanol	99.31
13	linear	61	400	yes	ethanol	98.00
14	cycles	61	400	yes	2-propanol	98.84
15	linear	550	400	yes	2-propanol	99.58
16	cycles	550	400	yes	ethanol	98.00

1  
2  
3 <sup>a</sup> Experimental details are described in the experimental section. <sup>b</sup> The output is the percentage PA in  
4 the solid phase.  
5  
6  
7  
8  
9

10 The input and output of the 16 tested experiments are tabulated in Table 1 and a Pareto chart  
11 (calculated using Minitab 18) in Figure 7 shows the effects from the tested factors and their  
12 combinations on the percentage of PA in the solid phase. The direction on how the parameters affect  
13 the purity of PA is shown in the main effects plot in Figure 8.  
14  
15  
16  
17

18 Shown in the Pareto chart is Lenth's pseudo standard error (PSE) at 0.4387, which separates  
19 the main effects from effects caused by random error. In the present work, the type of solvent, seeding  
20 and their combination have a significant effect on the purification of PA whereas the cooling method,  
21 cooling time and stirring rate are close to- or lower than Lenth's PSE. Therefore, the cooling method,  
22 cooling time and stirring parameters were not investigated further in this study.  
23  
24  
25  
26  
27

28 The type of solvent was the statistically most significant effect at a confidence level higher  
29 than 80%, closely followed by seeding. Interestingly, the use of seed crystals led to an average  
30 product purity of 98.59% as compared to an average product purity of 99.28% in unseeded  
31 experiments. The addition of seed crystals leads to a large crystal surface area across the bulk solution  
32 and a rapid depletion of supersaturation which may favour the incorporation of the CA impurities into  
33 the solid phase of PA. Without seed crystals, crystallization proceeds locally through primary  
34 nucleation followed by a slow depletion of supersaturation, possibly favouring the crystal growth of  
35 PA over impurity CA.  
36  
37  
38  
39  
40  
41  
42  
43  
44  
45  
46  
47  
48  
49  
50  
51  
52  
53  
54  
55  
56  
57  
58  
59  
60

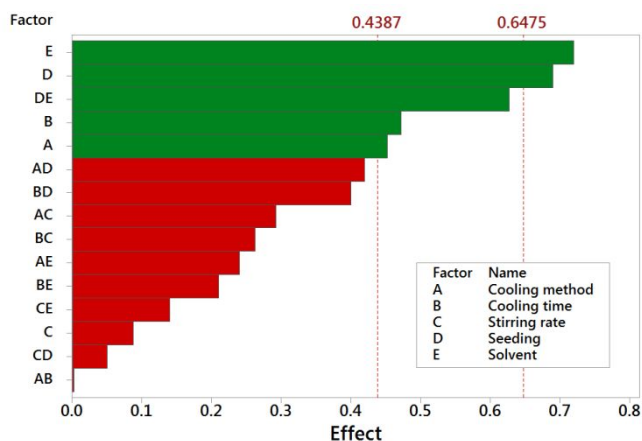


**Figure 7.** Pareto chart of the effects from the tested factors and their combinations, where the response is the percentage PA in the solid phase. Lenth's PSE is 0.4387 which separates the main effects from effects caused by random error. Effects that pass the vertical dashed line at 0.6475 are statistically significant at a confidence level of 80%.

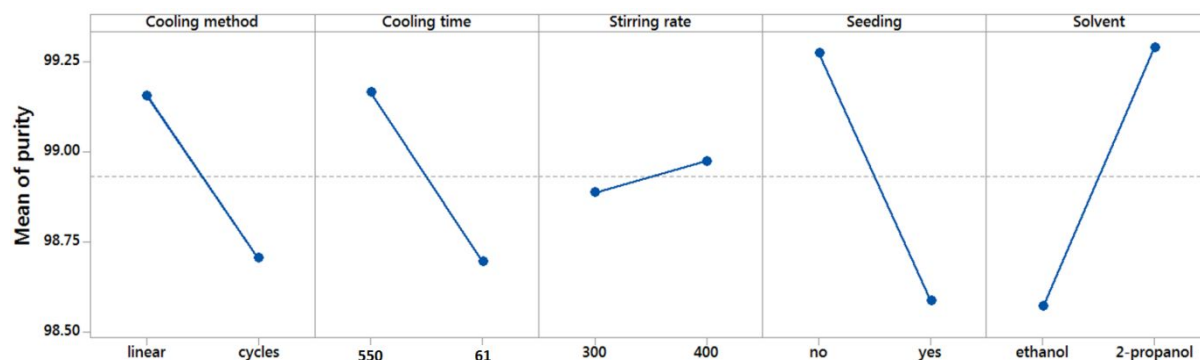


**Figure 8.** Main effects plots showing the direction the parameters affect the mean purity of PA.

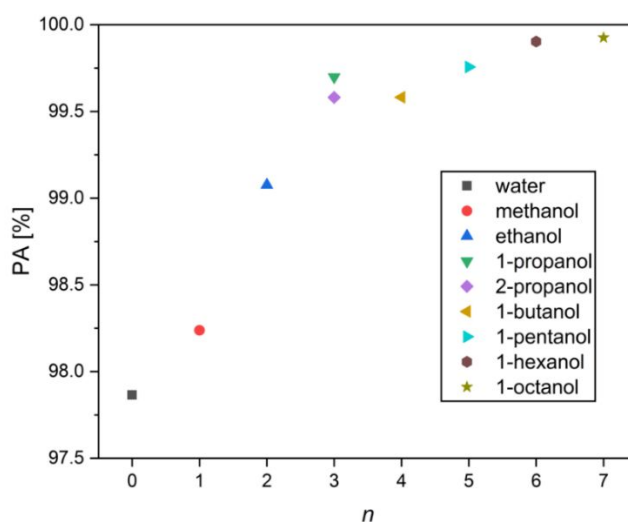
### 3.3.2. Solvent Selection

Based on the analysis from the previous section, the purity of PA is mainly affected by solvent selection. Therefore, the effect of solvent type on the purity of PA was explored in more detail. Water as well as eight different alcohols that varied in the number  $n$  of carbon atoms in the alkyl chain length were tested as solvents for recrystallization experiments. The dependence of the PA solid phase purity on the number  $n$  of carbon atoms in the alkyl chain length is plotted in Figure 9. Intriguingly, the incorporation of CA into the solid phase of PA strongly depends on the number  $n$  of carbon atoms in the alkyl chain length of the solvent as the purity of PA becomes higher with

1  
2  
3 increasing alcohol chain length. The crystal growth rate is possibly significantly reduced in alcohols  
4 with longer alkyl chain lengths. The reduced crystal growth rates may favour incorporation of PA  
5 over CA, resulting in higher purities of PA.  
6  
7  
8

9 The data for 1-propanol and 2-propanol slightly deviates from the observed general trend.  
10 This may be due to experimental errors as each data point represents a single experiment.  
11 Nevertheless, a clear relationship between the purity of PA and the number  $n$  of carbon atoms in the  
12 aliphatic chain of the alcohol solvent is apparent.  
13  
14  
15  
16

17 Thus, the amount of CA in the solid phase of PA can straightforwardly be controlled by  
18 solvent selection. The present work shows a correlation between the number  $n$  of carbon atoms in the  
19 aliphatic chain of the alcohol solvent and purity of a pharmaceutical product for the first time to the  
20 best of our knowledge. An increase in the number  $n$  of carbon atoms in the aliphatic chain of the  
21 alcohol solvent leads to an increase in PA purity. These results show that solvent selection can be  
22 used to accurately tailor the compressibility of PA as the amount of impurity in the solid phase of PA  
23 strongly impacts its compressibility.  
24  
25  
26  
27  
28  
29  
30  
31  
32  
33



34  
35  
36  
37  
38  
39  
40  
41  
42  
43  
44  
45  
46  
47  
48  
49  
50  
51  
52 **Figure 9.** PA purity as a function of the number  $n$  of carbons in the aliphatic chain of the alcohol  
53 solvent. A supersaturation ratio  $S$  of 1.71 and an initial 2 mol% of CA was used in all experiments.  
54  
55  
56  
57

#### 58 4. CONCLUSIONS

59  
60

1  
2  
3 Although significantly different in molecular structure and solubility, both impurity NP and  
4 CA slightly increased the solubility of PA and significantly reduced its nucleation rate in a similar  
5 fashion. The solid-liquid interfacial energy of PA remained unaffected by the impurities whereas the  
6 kinetic parameter was inhibited. The presence of CA in the solid phase of PA led to a striking increase  
7 in its compressibility resulting in favourable product specifications. An increase in the number of  
8 carbon atoms in the aliphatic chain of the alcohol solvent led to an increase in PA purity. Solvent  
9 selection could be used to tailor the product properties as shorter chain alcohols led to more efficient  
10 impurity incorporation and higher compressibility.  
11  
12  
13  
14  
15  
16  
17  
18  
19  
20

## 21 AUTHOR INFORMATION

### 22 **Corresponding Author**

23 \*E-mail: Leila.keshavarz@ul.ie  
24  
25  
26  
27  
28  
29

### 30 **ORCID**

31 René R. E. Steendam: 0000-0002-3363-4160

32 Leila Keshavarz: 0000-0002-1218-9352

33 Melian A. R. Blijlevens: 0000-0002-0566-4960

34 Patrick J. Frawley: 0000-0001-7066-0942  
35  
36  
37  
38  
39  
40  
41

### 42 **Funding**

43 This research has been conducted as part of the Synthesis and Solid State Pharmaceutical Centre  
44 (SSPC) and funded by Science Foundation Ireland (SFI) under Grant 12/RC/2275. We would like to  
45 acknowledge the Erasmus scheme and the Radboud University for exchange support (M. A. R. B.)  
46  
47  
48  
49  
50  
51  
52

### 53 **Notes**

54 The authors declare no competing financial interest.  
55  
56  
57  
58

## 59 REFERENCES

60

- 1
- 2
- 3 (1) Sangwal, K., Additives and Crystallization Processes: From Fundamentals to Applications. *Additives and Crystallization Processes: From Fundamentals to Applications* **2007**.
- 4
- 5 (2) Schmidt, C.; Jones, M. J.; Ulrich, J., The Influence of Additives and Impurities on
- 6 Crystallization. In *Crystallization*, Wiley-VCH Verlag GmbH & Co. KGaA: 2013; pp 105-127.
- 7
- 8 (3) Sun, C. C.; Sun, W.; Price, S.; Hughes, C.; Ter Horst, J.; Veesler, S.; Lewtas, K.; Myerson, A.;
- 9 Pan, H.; Coquerel, G.; van den Ende, J.; Meekes, H.; Mazzotti, M.; Rosbottom, I.; Taulelle, F.; Black,
- 10 S.; Mackenzie, A.; Janbon, S.; Vekilov, P.; Threlfall, T.; Turner, T.; Back, K.; Cuppen, H.; Toroz, D.;
- 11 Sefcik, J.; Lovelock, J.; Hammond, R.; Candoni, N.; Simone, E.; Ward, M.; Bertran, C. A.; Vetter, T.;
- 12 Sear, R.; De Yoreo, J.; Davey, R.; Anwar, J.; Santiso, E.; Wu, D. T.; Roberts, K.; Peters, B.; Schroeder, S.;
- 13 Jones, F.; Rasmuson, A.; Cölfen, H.; Zeglinski, J.; Salvalaglio, M., Solvent and additive interactions as
- 14 determinants in the nucleation pathway: general discussion. *Faraday Discuss.* **2015**, 179, 383-420.
- 15
- 16 (4) Singh, S., The last decade in regulation and control of impurities in pharmaceuticals. *Trends*
- 17 *Anal. Chem.* **2018**, 101, 1.
- 18
- 19 (5) Peng, J.; Dong, Y.; Wang, L.; Li, L.; Li, W.; Feng, H., Effect of Impurities on the Solubility,
- 20 Metastable Zone Width, and Nucleation Kinetics of Borax Decahydrate. *Ind. Eng. Chem. Res.* **2014**,
- 21 53, 12170-12178.
- 22
- 23 (6) Song, R.-Q.; Colfen, H., Additive controlled crystallization. *CrystEngComm* **2011**, 13, 1249-
- 24 1276.
- 25
- 26 (7) Pino-García, O.; Rasmuson, Å. C., Influence of Additives on Nucleation of Vanillin:
- 27 Experiments and Introductory Molecular Simulations. *Cryst. Growth Des.* **2004**, 4, 1025-1037.
- 28
- 29 (8) Anwar, J.; Boateng, P. K.; Tamaki, R.; Odedra, S., Mode of Action and Design Rules for
- 30 Additives That Modulate Crystal Nucleation. *Angew. Chem. Int. Ed.* **2009**, 48, 1596-1600.
- 31
- 32 (9) Kim, J.-W.; Park, J.-H.; Shim, H.-M.; Koo, K.-K., Effect of Amphiphilic Additives on Nucleation
- 33 of Hexahydro-1,3,5-trinitro-1,3,5-triazine. *Cryst. Growth Des.* **2013**, 13, 4688-4694.
- 34
- 35 (10) Bodnár, K.; Hudson, S. P.; Rasmuson, Å. C., Promotion of Mefenamic Acid Nucleation by a
- 36 Surfactant Additive, Docusate Sodium. *Cryst. Growth Des.* **2018**, 19, 591-603.
- 37
- 38 (11) Poornachary, S. K.; Han, G.; Kwek, J. W.; Chow, P. S.; Tan, R. B. H., Crystallizing Micronized
- 39 Particles of a Poorly Water-Soluble Active Pharmaceutical Ingredient: Nucleation Enhancement by
- 40 Polymeric Additives. *Cryst. Growth Des.* **2016**, 16, 749-758.
- 41
- 42 (12) Heffernan, C.; Ukrainczyk, M.; Zeglinski, J.; Hodnett, B. K.; Rasmuson, A. C., The Influence of
- 43 Structurally-Related Impurities on the Crystal Nucleation of Curcumin. *Cryst. Growth Des.* **2018**, 18,
- 44 4715-4723.
- 45
- 46 (13) Pons Siepermann, C. A.; Myerson, A. S., Inhibition of Nucleation Using a Dilute, Weakly
- 47 Hydrogen-Bonding Molecular Additive. *Cryst. Growth Des.* **2018**, 18, 3584-3595.
- 48
- 49 (14) Kaialy, W.; Larhrib, H.; Chikwanha, B.; Shojaee, S.; Nokhodchi, A., An approach to engineer
- 50 paracetamol crystals by antisolvent crystallization technique in presence of various additives for
- 51 direct compression. *Int. J. Pharm.* **2014**, 464, 53-64.
- 52
- 53 (15) Garekani, H. A.; Ford, J. L.; Rubinstein, M. H.; Rajabi-Siahboomi, A. R., Highly compressible
- 54 paracetamol — II. Compression properties. *Int. J. Pharm.* **2000**, 208, 101-110.
- 55
- 56 (16) Haisa, M.; Kashino, S.; Kawai, R.; Maeda, H., The Monoclinic Form of p-Hydroxyacetanilide.
- 57 *Acta Crystallogr. B* **1976**, 32, 1283-1285.
- 58
- 59 (17) Drebuschak Tatyana, N.; Boldyreva Elena, V., Variable temperature (100–360 K) single-
- 60 crystal X-ray diffraction study of the orthorhombic polymorph of paracetamol (p-
- hydroxyacetanilide). In *Zeitschrift für Kristallographie - Crystalline Materials*, ed. **2004**, 219, 506.
- (18) Perrin, M.-A.; Neumann, M. A.; Elmaleh, H.; Zaske, L., Crystal structure determination of the
- elusive paracetamol Form III. *ChemComm* **2009**, 3181-3183.
- (19) Hendriksen, B. A.; Grant, D. J. W.; Meenan, P.; Green, D. A., Crystallisation of paracetamol
- (acetaminophen) in the presence of structurally related substances. *J. Cryst. Growth* **1998**, 183, 629-
- 640.
- (20) Prasad, K. V. R.; Ristic, R. I.; Sheen, D. B.; Sherwood, J. N., Crystallization of paracetamol from
- solution in the presence and absence of impurity. *Int. J. Pharm.* **2001**, 215, 29-44.

- 1  
2  
3 (21) Saleemi, A.; Onyemelukwe, I. I.; Nagy, Z., Effects of a structurally related substance on the  
4 crystallization of paracetamol. *Front. Chem. Sci. Eng.* **2013**, *7*, 79-87.
- 5 (22) Nguyen, T.; Khan, A.; Bruce, L.; Forbes, C.; O'Leary, R.; Price, C., The Effect of Ultrasound on  
6 the Crystallisation of Paracetamol in the Presence of Structurally Similar Impurities. *Crystals* **2017**, *7*,  
7 294.
- 8 (23) Santa Cruz Biotechnology, I. MSDS. <http://datasheets.scbt.com/sc-206922.pdf>
- 9 (24) Board, N., *Drugs & Pharmaceutical Technology Handbook*. ed.; Asia Pacific Buisness Press  
10 Inc.: **2004**.
- 11 (25) According to the SDS sheet on the Website of Sigma Aldrich, 4'-chloroacetanilide is not a  
12 hazardous substance or mixture according to Regulation (EC) No. 1272/2008
- 13 (26) Sato, H.; Watanabe, S.; Takeda, D.; Yano, S.; Doki, N.; Yokota, M.; Shimizu, K., Optimization  
14 of a Crystallization Process for Orantinib Active Pharmaceutical Ingredient by Design of Experiment  
15 To Control Residual Solvent Amount and Particle Size Distribution. *Org. Proc. Res. & Dev.* **2015**, *19*,  
16 1655-1661.
- 17 (27) de Souza, B.; Keshavarz, L.; Steendam, R. R. E.; Dennehy, O. C.; Lynch, D.; Collins, S. G.;  
18 Moynihan, H. A.; Maguire, A. R.; Frawley, P. J., Solubility Measurement and Thermodynamic  
19 Modeling of N-(4-Methylphenyl-Z-3-chloro-2-(phenylthio)propenamide in 12 Pure Solvents at  
20 Temperatures Ranging from 278.15 to 318.15 K. *J. Chem. Thermodyn.* **2018**, *63*, 1419-1428.
- 21 (28) Capello, C.; Fischer, U.; Hungerbuhler, K., What is a green solvent? A comprehensive  
22 framework for the environmental assessment of solvents. *Green Chem.* **2007**, *9*, 927-934.
- 23 (29) Granberg, R. A.; Rasmuson, A. C., Solubility of paracetamol in pure solvents. *J Chem Eng Data*  
24 **1999**, *44*, 1391-1395.
- 25 (30) mol% impurity relative to PA only
- 26 (31) Wu, Z.; Yang, S.; Wu, W., Application of temperature cycling for crystal quality control during  
27 crystallization. *CrystEngComm* **2016**.
- 28 (32) Keshavarz, L.; Steendam, R. R. E.; Frawley, P. J., Impact of Mother Liquor Recycle on the  
29 Impurity Buildup in Crystallization Processes. *Org. Proc. Res. & Dev.* **2018**, *22*, 1541-1547.
- 30 (33) Steendam, R. R. E.; Keshavarz, L.; de Souza, B.; Frawley, P. J., Thermodynamic properties of  
31 paracetamol impurities 4-nitrophenol and 4'-chloroacetanilide and the impact of such impurities on  
32 the crystallisation of paracetamol from solution. *J. Chem. Thermodyn.* **2019**, *133*, 85-92.
- 33 (34) Pishnamazi, M.; Casilagan, S.; Clancy, C.; Shirazian, S.; Iqbal, J.; Egan, D.; Edlin, C.; Croker, D.  
34 M.; Walker, G. M.; Collins, M. N., Microcrystalline cellulose, lactose and lignin blends: Process  
35 mapping of dry granulation via roll compaction. *Powder Technol.* **2019**, *341*, 38-50.
- 36 (35) Ottoboni, S.; Chrubasik, M. M.; Mir Bruce, L.; Nguyen, T. T. H.; Robertson, M.; Johnston, B.;  
37 Oswald, I. D. H.; Florence, A.; Price, C., Impact of Paracetamol Impurities on Face Properties:  
38 Investigating the Surface of Single Crystals Using TOF-SIMS. *Cryst. Growth Des.* **2018**, *18*, 2750-2758.
- 39 (36) de Souza, B.; Keshavarz, L.; Cogoni, G.; Frawley, P. J., Pressurized-Synthetic Methodology for  
40 Solubility Determination at Elevated Temperatures with Application to Paracetamol in Pure Solvents.  
41 *J. Chem. Eng. Data* **2017**, *62*, 1689-1700.
- 42 (37) S. Jiang, S.; ter Horst, J. H., Crystal Nucleation Rates from Probability Distributions of  
43 Induction Times. *Cryst. Growth Des.* **2011**, *11*, 256-261.
- 44 (38) Steendam, R. R. E.; Keshavarz, L.; Blijlevens, M. A. R.; de Souza, B.; Croker, D. M.; Frawley, P.  
45 J., Effects of Scale-Up on the Mechanism and Kinetics of Crystal Nucleation. *Cryst. Growth Des.* **2018**,  
46 *18*, 5547-5555.
- 47 (39) Xiao, Y.; Tang, S. K.; Hao, H.; Davey, R. J.; Vetter, T., Quantifying the Inherent Uncertainty  
48 Associated with Nucleation Rates Estimated from Induction Time Data Measured in Small Volumes.  
49 *Cryst. Growth Des.* **2017**, *17*, 2852-2863.
- 50 (40) Davey, R. J.; Schroeder, S. L. M.; ter Horst, J. H., Nucleation of Organic Crystals—A Molecular  
51 Perspective. *Angew. Chem. Int. Ed.* **2013**, *52*, 2166-2179.
- 52 (41) Kulkarni, S. A.; Weber, C. C.; Myerson, A. S.; ter Horst, J. H., Self-Association during  
53 Heterogeneous Nucleation onto Well-Defined Templates. *Langmuir* **2014**, *30*, (41), 12368-12375.
- 54  
55  
56  
57  
58  
59  
60



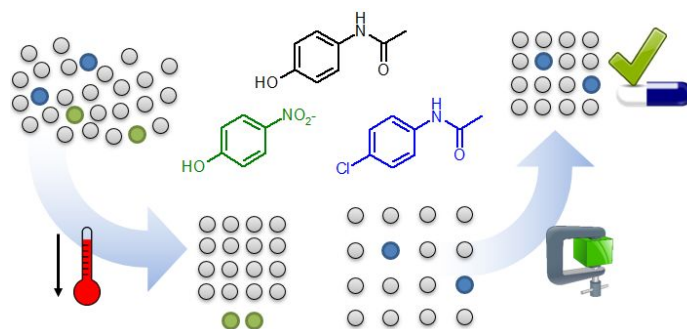
(42) Naumov, D. Y.; Vasilchenko, M. A.; Howard, J. A. K., The Monoclinic Form of Acetaminophen at 150K. *Acta Crystallogr. A* **1998**, 54, 653-655.

(43) Ukrainczyk, M.; Hodnett, B. K.; Rasmuson, Å. C., Process Parameters in the Purification of Curcumin by Cooling Crystallization. *Org. Proc. Res. & Dev.* **2016**, 20, 1593-1602.

## For Table of Contents Use Only

### Influence of Impurities on the Solubility, Nucleation, Crystallization and Compressibility of Paracetamol

Leila Keshavarz<sup>†\*</sup>, René R. E. Steendam<sup>†</sup>, Lian Blijlevens, Mahboubeh Pishnamazi and Patrick J. Frawley



Impurities 4-nitrophenol and 4'-chloroacetanilide increase the solubility and inhibit the nucleation of paracetamol in the same way, despite their differences in molecular structure, solubility and ability to incorporate into the solid phase of paracetamol. Incorporation of 4'-chloroacetanilide into paracetamol can be controlled through solvent choice and the resulting crystal product was significantly improved in terms of compressibility.